ACS Catalysis

Research Article

pubs.acs.org/acscatalysis

Investigating the Plasmon-Mediated Catalytic Activity of AgAu Nanoparticles as a Function of Composition: Are Two Metals Better than One?

J. L. Wang, Romulo A. Ando, and Pedro H. C. Camargo*

Departamento de Química Fundamental, Instituto de Química, Universidade de São Paulo, Av. Prof. Lineu Prestes, 748, 05508-000 São Paulo-SP, Brazil

Supporting Information

ABSTRACT: The surface plasmon resonance (SPR) excitation by visible light in plasmonic nanostructures can be put to work to mediate catalytic processes. However, the role of composition in bimetallic nanoparticles over the SPR-mediated catalytic activity remains unclear. We investigated herein the SPR-mediated catalytic activity of AgAu nanoparticles as a function of composition toward the oxidation of *p*-aminothiophenol to *p,p′*-dimercaptoazobenzene. Our results showed that a "volcano-type" relationship between composition and product conversion was observed, with a maximum activity observed for $Ag_{0.19}Au_{0.81}$ nanoparticles. The variations in catalytic activity could be explained by the balance between the matching of the excitation wavelength with SPR position and the plasmonic damping due to interband transitions above 500 nm. These data suggest that the precise control over composition allows the fine-tuning of catalytic activity in SPR-mediated catalytic processes.

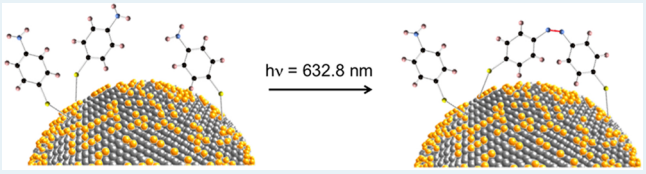

KEYWORDS: *nanoparticles, bimetallic, silver, gold, SPR, plasmon-mediated catalysis, SERS*

INTRODUCTION

Gold nanoparticles (Au NPs) display remarkable optical properties in the visible range as a result of the excitation of their surface plasmon resonance (SPR) as well as catalytic activity toward a myriad of chemical transformations owing to their large surface-to-volume ratios.[1−4] However, when applications in catalysis are regarded, several examples have been demonstrated in which bimetallic nanoparticles have superior catalytic activity relative to their monometallic counterparts due to the synergism between the metal components.[5,6] In fact, a volcano-type relationship between composition and catalytic activity has been reported for many bimetallic systems and assigned to electronic and/or geometric effects.[7,8]

Plasmon-enhanced or plasmon-mediated transformations (SPR-enhanced or SPR-mediated catalysis) represent a new frontier in heterogeneous catalysis, in which light is employed as a sustainable energy input to drive chemical reactions.[8−10] Plasmonic nanostructures, such as silver (Ag) and gold (Au) NPs, can strongly interact with visible light as a result the SPR excitation, which consists of the collective oscillation of their conduction electrons at a characteristic frequency in response to an oscillating electric field from an incoming electromagnetic radiation (light).[10] In the context of catalysis, the SPR excitation can be put to work for enhancing or mediating chemical transformations by several mechanisms including the following: (i) by increasing the local electric field close to the nanostructure surface that enhances absorption at the metal-molecule interface; (ii) by generating electron−hole pairs that enable the occurrence of a charge-transfer process at the metal−molecule interface; and (iii) by generating local heating at the metal surface that provide energy for photothermal conversions.[10−12] Although several successful examples on the SPR-mediated chemical reactions have been described, most studies have been focused on the utilization of monometallic Ag or Au NPs, or the elucidation of reaction mechanisms.[13−16] Even though bimetallic NPs have been widely investigated in the context of heterogeneous catalysis, their role in SPR-mediated catalytic processes is still unclear. For instance, would they display better SPR-mediated catalytic activities relative to their monometallic counterparts? How would the SPR-mediated catalytic activities vary as a function of composition? Would they display a volcano-type relationship between composition and activity as observed in heterogeneous catalysts?

Some studies with regard to AgAu NPs associated with semiconducting materials have shown higher photodegradation rates than their monometallic counterparts under visible light illumination.[17] In these systems, it is generally accepted that the SPR-mediated catalytic activities are maximized when the excitation wavelength matches the SPR position.[18] In this paper, we investigated the SPR-mediated catalytic activity as a function of composition employing individual AgAu NPs as catalysts for the oxidation of *p*-aminothiophenol (PATP) to

Received: August 13, 2014
Revised: September 17, 2014
Published: September 18, 2014

p,*p*′-dimercaptoazobenzene (DMAB) by activated $^3O_2$ as a model reaction.[15,16] More specifically, we investigated the effect of the Au content in the NPs over the conversion of PATP to DMAB mediated by the SPR excitation, and we compared these results with those obtained for monometallic Ag and Au NPs. AgAu NPs displaying controlled compositions, spherical shapes, and relatively uniform sizes were synthesized by a facile coreduction approach.[19] They were chosen as catalysts because it is well-known that the optical properties (wavelength for the SPR excitation) in these systems can be tuned as a function of composition, enabling a precise correlation between composition (optical properties) and SPR-mediated catalytic activities.[20] Moreover, AgAu NPs also display improved catalytic activities relative to their monometallic counterparts, and light excitation may provide a further means of manipulating/optimizing catalytic activity in these systems.[7,12]

RESULTS AND DISCUSSION

We started our investigations with the synthesis of AgAu NPs with controlled compositions by a coreduction approach employing $AgNO_3$ and $HAuCl_4$ as the Ag and Au precursors, respectively, and sodium citrate as both the reducing agent and stabilizer (see Supporting Information for experimental details).[19] In this case, the composition in the AgAu NPs was controlled by manipulating the $Ag^+/AuCl_4^-$ molar ratios during the synthesis to give Ag, $Ag_{0.80}Au_{0.20}$, $Ag_{0.67}Au_{0.33}$, $Ag_{0.48}Au_{0.52}$, $Ag_{0.35}Au_{0.65}$, $Ag_{0.19}Au_{0.81}$, $Ag_{0.07}Au_{0.93}$, and Au NPs (these compositions were determined by FAAS − flame atomic absorption spectrometry). Figure 1a−h display SEM and TEM

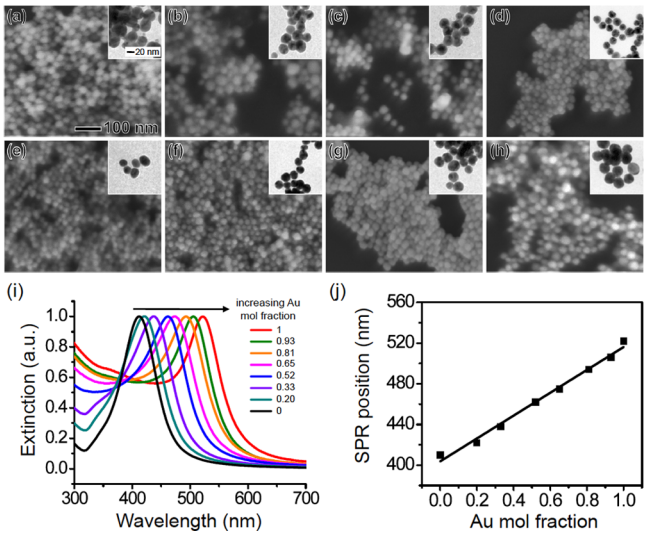

Figure 1. (a−h) SEM and TEM (inset) images for Ag (a), $Ag_{0.80}Au_{0.20}$ (b), $Ag_{0.67}Au_{0.33}$ (c), $Ag_{0.48}Au_{0.52}$ (d), $Ag_{0.35}Au_{0.65}$ (e), $Ag_{0.19}Au_{0.81}$ (f), $Ag_{0.07}Au_{0.93}$ (g), and Au NPs (h). UV−vis extinction spectra (i) and SPR peak positions (j) as a function of the Au content (Au mole fraction) in the NPs. The scale bars in (a) apply to all images/insets.

(insets) images for the obtained Ag, AgAu, and Au NPs. All NPs displayed spherical shapes and relatively uniform sizes, corroborating the formation of bimetallic systems rather than a mixture of monometallic NPs. Also, the absence of mass thickness contrast within individual AgAu NPs in the TEM images (insets) suggests the formation of AgAu alloys rather than core−shell architectures. Figure S1 depicts the Ag, AgAu, and Au NP diameters as a function of the Au mole fraction. In agreement with previous reports, the diameter of the NPs gradually decreased from 32 to 21 nm as the Au mole fraction increased from 0 to 0.52, respectively, and then gradually increased up to 30 nm as the Au mole fraction increased from 0.52 to 1.[19] Figure 1i depicts the UV−vis extinction spectra registered from aqueous suspensions containing the AgAu NPs as a function of the Au mole fraction (together with those obtained for monometallic Ag and Au NPs). Only one extinction band assigned to the dipole plasmon resonance excitation was observed in the spectra,[21] in which the maximum SPR position displayed a linear red shift from 410 nm (Ag NPs) to 522 nm (Au NPs) with the increase Au content (Figure 1j). This is also in agreement with the formation of AgAu alloyed NPs as opposed to monometallic or core−shell systems.[22−24]

After the synthesis of AgAu NPs displaying controlled compositions and optical properties, we turned our attention to the investigation of the effect of composition over their catalytic activity toward the SPR-mediated oxidation of PATP to DMAB by activated $^3O_2$ as depicted in Scheme 1. The utilization of this

Scheme 1. SPR-Mediated Oxidation of PATP to DMAB by $^3O_2$ Employing AgAu NPs as Catalysts[a]

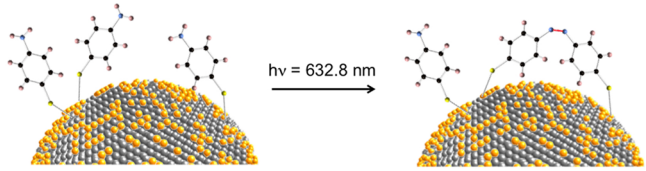

[a]PATP molecules strongly bind to the Ag and Au surface via Ag−S and Au−S covalent bonds. Upon irradiation, Ag−S and Au−S bonds are not broken as PATP molecules are converted to DMAB. Here, a laser irradiation (632.8 nm) using a Raman spectrophotometer is employed as the excitation source as well as to monitor the product conversion by the SERS effect.

reaction as a model to probe SPR-mediated catalytic activity was due to several aspects. First, PATP can bind strongly to Ag and Au surfaces via the formation of Ag−S or Au−S covalent bonds, which are not broken upon PATP oxidation to yield DMAB.[11,14,15] Also, this transformation can be easily performed and monitored using a Raman spectrometer, in which the incident laser can be employed both as the SPR excitation source and to probe the product conversion by the SERS effect, as PATP and DMAB display characteristic Raman bands at distinct spectral positions.[14−16] Finally, the mechanism for the selective oxidation of PATP to DMAB by activated $^3O_2$ upon SPR excitation has been recently established according to the following equation:[15]

$$2AuS - Ph - NH_2 + {}^3O_2 + hv \rightarrow AuS - Ph - N = N - Ph - SAu + 2H_2O \quad (1)$$

We chose to employ 632.8 nm as the excitation wavelength as it has been show that the yield of DMAB follows the order of 632.8 nm > 785 nm > 532 nm.[15] In this case, the SPR excitation by the incoming light results in the formation of hot electrons that can be transferred from the nanoparticle to adsorbed $^3O_2$ (from air) to produce strongly adsorbed $^2O_2^-$ species at the nanoparticle surface. Although $^2O_2^-$ can contribute to the PATP oxidation, local heating as a result of the SPR excitation may also lead to the formation of surface Ag or Au oxides and hydroxides species that can further oxidize

dx.doi.org/10.1021/cs501189m | ACS Catal. 2014, 4, 3815−3819

PATP. Therefore, the $^3O_2$ activation driven by the SPR excitation play a pivotal role over this transformation, and we were interested in investigating how this transformation was dependent on the composition of AgAu NPs.

Figure 2 displays the irradiation-time-dependent SERS spectra of $Ag_{0.19}Au_{0.81}$ NPs functionalized with PATP acquired

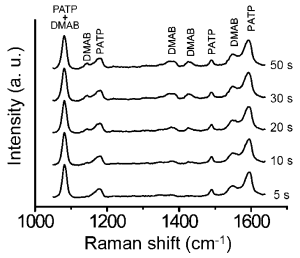

Figure 2. Irradiation-time-dependent SERS spectra acquired for $Ag_{0.19}Au_{0.81}$ NPs functionalized with PATP employing 0.015 mW as the laser irradiation power. The spectra were recorded under 633 nm excitation, and all intensities were normalized with respect to the signal at 1081 cm^{-1}.

at a 0.015 mW laser power. Our results clearly show the selective oxidation of PATP to DMAB by $^3O_2$ mediated by SPR excitation due to the appearance of the bands at 1142, 1390, 1433, and 1575 cm^{-1} assigned to the A_g modes of DMAB.[25,26] The bands at 1081, 1188, 1489, and 1593 cm^{-1} are assigned to A_1 modes of PATP.[25,26] In this case, the product conversion can be detected by monitoring the DMAB/PATP intensity ratios.[14−16] It can be clearly observed that the Raman intensities assigned to DMAB increase with the laser irradiation time. However, when the exposure time increased from 30 to 50 s (or more), no significant changes in the relative DMAB/PATP intensity ratios were observed. As longer laser exposure times may result in the damage of probe molecules, we decided to use the 30 s irradiation time for all subsequent measurements.

In order to confirm that the conversion was mediated by the SPR effect, we studied the laser-power-dependent SERS spectra of $Ag_{0.19}Au_{0.81}$ NPs functionalized with PATP as depicted in Figure 3a. Figure 3b shows the DMAB/PATP 1433/1593 cm^{-1} intensity ratios as a function of the laser power. It can be observed that the relative Raman intensities of A_g modes corresponding to DMAB as well as the DMAB/PATP 1433/1593 cm^{-1} intensity ratios increased steadily with the laser power, in agreement with a SPR-mediated reaction mechanism, as stronger light intensities will induce a larger population of electrons at higher energy levels (that can be transferred to molecules adsorbed at the surface), create a stronger electromagnetic field around the NPs, and/or induce higher local heating at the proximity of the NPs surface.[10]

Figure 4a shows the SERS spectra of Ag, AgAu, and Au NPs functionalized with PATP nanoparticles as a function of the Au mole fraction and employing 0.13 mW as the laser irradiation power. The DMAB/PATP intensity ratios were calculated employing the 1433/1593 cm^{-1} Raman intensities and are shown in Figure 4b. Our results indicated that the DMAB/PATP intensity ratios and thus the SPR-mediated catalytic activity displayed a strong dependence with respect to the compositional variations of the NPs. While the relative signal intensities and DMAB/PATP intensity ratios did not significantly change as the Au mole fraction in the NPs was increased from 0 to 0.20, they increased when the Au mole fraction was above 0.20. Specifically, the DMAB/PATP

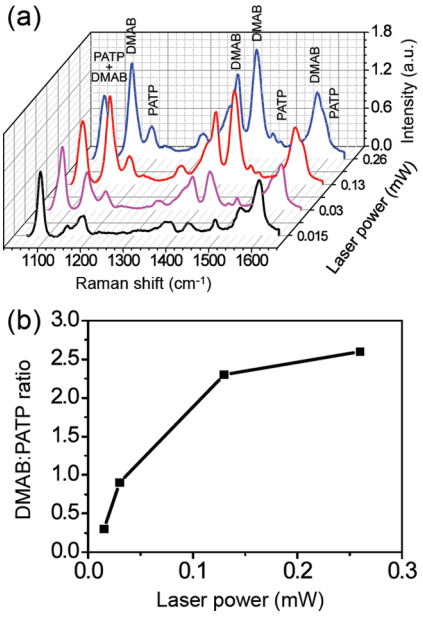

Figure 3. (a) Laser-power-dependent SERS spectra of $Ag_{0.19}Au_{0.81}$ NPs functionalized with PATP employing 30 s as the exposure time. (b) Obtained DMAB/PATP 1433/1593 cm^{-1} intensity ratios as a function of the laser power. The spectra were recorded under 633 nm excitation, and all intensities were normalized with respect to the signal at 1081 cm^{-1}.

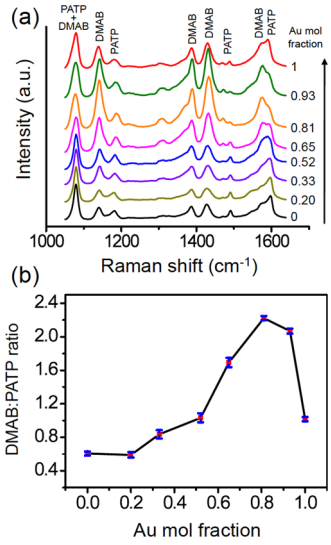

Figure 4. (a) SERS spectra as a function of composition (Au mole fraction) employing Ag, $Ag_{0.80}Au_{0.20}$, $Ag_{0.67}Au_{0.33}$, $Ag_{0.48}Au_{0.52}$, $Ag_{0.35}Au_{0.65}$, $Ag_{0.19}Au_{0.81}$, $Ag_{0.07}Au_{0.93}$, and Au NPs functionalized with PATP. (b) Obtained DMAB/PATP 1433/1593 cm^{-1} intensity ratios as a function of the Au content in the NPs. The spectra were recorded under 633 nm excitation, and all intensities were normalized with respect to the signal at 1081 cm^{-1}.

intensity ratios corresponded to 0.84, 1.03, and 1.69 for 0.33, 0.52, and 0.65 Au mole fractions, respectively. Interestingly, a peak in the DMAB/PATP intensity ratios at 2.22 was detected as the Au mole fraction corresponded to 0.81, followed by a decrease to 2.07 and 1.02 as the Au mole fraction was further increased to 0.93 and 1 (monometallic Au NPs). These results indicate that bimetallic NPs having $Ag_{0.35}Au_{0.65}$, $Ag_{0.19}Au_{0.81}$, and $Ag_{0.07}Au_{0.93}$ compositions displayed higher SPR-mediated

dx.doi.org/10.1021/cs501189m | ACS Catal. 2014, 4, 3815−3819

catalytic activity as compared to their monometallic counterparts (Ag and Au NPs). Moreover, as often described for heterogeneous catalysts and electrocatalysts, our results indicate a "volcano-type" relationship between chemical composition and SPR-mediated catalytic activity of AgAu NPs toward the oxidation of PATP.

The observed variations in the catalytic activity as a function of the composition can be explained by two factors that influence SPR excitation: (i) the matching between the excitation wavelength and the SPR position and (ii) the damping of plasmon oscillation due to Au interband transitions above ∼500 nm. Although an increased matching between excitation wavelength and SPR position lead to stronger plasmon excitation, which enable the generation of a larger population of hot electrons[27] (that can be transferred to $^3O_2$) as well as higher localized heating close to the NPs surface, interband transitions hamper the generation of hot electrons and local heating at the nanoparticle surface. As the Au mole fractions in the AgAu NPs varied from 0 (Ag NPs) to 0.81, the SPR position red-shifted from 410 to 494 nm, implying an increased matching with the 633 nm excitation wavelength and thus a stronger plasmon oscillation, which enable a higher SPR-mediated catalytic activity toward the oxidation of PATP. As the Au mole fraction further increases to 0.93 and 1 (Au NPs), the SPR wavelength further red-shifted to 506 and 522 nm, respectively. For Ag, the interband transitions have an edge at 3.8 eV, and this value reduces as the Au molar fraction in the AgAu nanoparticles increases until it reaches at 2.5 eV for Au.[28] Thus, in these wavelengths, Au interband transitions start to become an effective pathway for the damping of the plasmon oscillation.[29] In this case, although an increased matching is observed between the SPR and the excitation wavelength, the contribution of the interband transitions to the damping of plasmon oscillation is strong enough to lead to a decrease in the SPR-mediated catalytic activity. Therefore, we believe that the "volcano-type" relationship between chemical composition and SPR-mediated catalytic activity in AgAu bimetallic nanoparticles was dependent on the SPR excitation wavelength of the NPs, its matching with the excitation wavelength, and plasmon damping mechanisms (such as interband transitions). It is important to note that surfaces with different Au/Ag composition may have different interactions with oxygen, which could also affect the catalytic performances. However, it is plausible that these differences in surface sensitivity do not play the major role over the observed variations in the catalytic performance, as the SPR-mediated catalytic activity for some AgAu bimetallic compositions were much higher relative to either monometallic Ag or Au NPs.

CONCLUSIONS

In summary, we described a systematic study on the effect of composition (Au mole fraction) in AgAu NPs over their SPR-mediated catalytic activity toward the oxidation of PATP to DMAB by activated $^3O_2$. The Ag, $Ag_{0.80}Au_{0.20}$, $Ag_{0.67}Au_{0.33}$, $Ag_{0.48}Au_{0.52}$, $Ag_{0.35}Au_{0.65}$, $Ag_{0.19}Au_{0.81}$, $Ag_{0.07}Au_{0.93}$, and Au NPs employed as catalysts displayed relatively spherical shapes, uniform sizes, and their SPR band position gradually red-shifted from 410 to 522 nm as the Au mole fraction in the NPs was increased from 0 (in Ag NPs) to 1 (in Au NPs). Our results showed that the SPR-mediated catalytic activity was strongly dependent on composition. In addition to $Ag_{0.35}Au_{0.65}$, $Ag_{0.19}Au_{0.81}$, and $Ag_{0.07}Au_{0.93}$ NPs having higher catalytic activities than Ag and Au NPs (monometallic systems), a "volcano-type" relationship between chemical composition and catalytic activity was observed, with a peak for the $Ag_{0.19}Au_{0.81}$ composition. The variations in the SPR-mediated catalytic activity could be explained by the balance between the matching of the excitation wavelength with the SPR position, that lead to stronger plasmon excitations, and the plasmonic damping due to interband transitions above 500 nm. As observed and described for heterogeneous catalysts and electrocatalysts, these results suggest that the precise control over composition allows the fine-tuning of catalytic activity in SPR-mediated catalytic processes.

ASSOCIATED CONTENT

Supporting Information

Experimental details and size of the Ag, Au, and AgAu NPs, and additional spectra. This material is available free of charge via the Internet at http://pubs.acs.org.

AUTHOR INFORMATION

Corresponding Author

*E-mail: camargo@iq.usp.br.

Notes

The authors declare no competing financial interest.

ACKNOWLEDGMENTS

This work was supported by the Fundação de Amparo à Pesquisa do Estado de São Paulo (FAPESP) (grant no. 2013/19861-6) and the Conselho Nacional de Desenvolvimento Científico e Tecnológico (CNPq) (grant no. 471245/2012-7). P.H.C.C. and R.A.A. thank the CNPq for research fellowships. J.W. thanks FAPESP for the fellowship (2013/05709-8).

REFERENCES

(1) Christensen, C. H.; Norskov, J. K. *Science* **2010**, *327*, 278−279.
(2) Daniel, M.-C.; Astruc, D. *Chem. Rev.* **2004**, *104*, 293−346.
(3) Buurmans, I. L. C.; Weckhuysen, B. M. *Nat. Chem.* **2012**, *4*, 873−886.
(4) Kim, H.; Kosuda, K. M.; Van Duyne, R. P.; Stair, P. C. *Chem. Soc. Rev.* **2010**, *39*, 4820−4844.
(5) Sankar, M.; Dimitratos, N.; Miedziak, P. J.; Wells, P. P.; Kiely, C. J.; Hutchings, G. J. *Chem. Soc. Rev.* **2012**, *41*, 8099−8139.
(6) Alonso, D. M.; Wettsteinab, S. G.; Dumesic, J. A. *Chem. Soc. Rev.* **2012**, *41*, 8075−8098.
(7) Slater, T. J. A.; Macedo, A.; Schroeder, S. L. M.; Burke, M. G.; O'Brien, P.; Camargo, P. H. C.; Haigh, S. J. *Nano Lett.* **2014**, *14*, 1921−1926.
(8) Sarina, S.; Zhu, H. Y.; Jaatinen, E.; Xiao, Q.; Liu, H. W.; Jia, J. F.; Chen, C.; Zhao, J. *J. Am. Chem. Soc.* **2013**, *135*, 5793−5801.
(9) Kale, M. J.; Avanesian, T.; Christopher, P. *ACS Catal.* **2014**, *4*, 116−128.
(10) Baffoua, G.; Quidant, R. *Chem. Soc. Rev.* **2014**, *43*, 3898−3907.
(11) Huang, Y.-F.; Wu, D.-Y.; Zhu, H.-P.; Zhao, L.-B.; Liu, G.-K.; Ren, B.; Tian, Z.-Q. *Phys. Chem. Chem. Phys.* **2012**, *14*, 8485−8497.
(12) Gonzalez-Bejar, M.; Peters, K.; Hallett-Tapley, G. L.; Grenierb, M.; Scaiano, J. C. *Chem. Commun.* **2013**, *49*, 1732−1734.
(13) Wu, D. Y.; Liu, X. M.; Huang, Y. F.; Ren, B.; Xu, X.; Tian, Z. Q. *J. Phys. Chem. C* **2009**, *113*, 18212−18222.
(14) Huang, Y. F.; Zhu, H. P.; Liu, G. K.; Wu, D. Y.; Ren, B.; Tian, Z. Q. *J. Am. Chem. Soc.* **2010**, *132*, 9244−9246.
(15) Huang, Y.-F.; Zhang, M.; Zhao, L.-B.; Feng, J.-M.; Wu, D.-Y.; Ren, B.; Tian, Z.-Q. *Angew. Chem., Int. Ed.* **2014**, *126*, 1−6.
(16) Zhao, L.-B.; Zhang, M.; Huang, Y.-F.; Williams, C. T.; Wu, D.-Y.; Ren, B.; Tian, Z.-Q. *J. Phys. Chem. Lett.* **2014**, *5*, 1259−1266.
(17) Zielińska-Jurek, A.; Kowalska, E.; Sobczak, J. W.; Lisowski, W.; Ohtani, B.; Zaleska, A. *Appl. Catal., B* **2011**, *101*, 504−514.

(18) Verbruggen, S. W.; Keulemans, M.; Filippousi, M.; Flahaut, D.; Van Tendeloo, G.; Lacombe, S.; Martens, J. A.; Lenaerts, S. *Appl. Catal., B* **2014**, *156−157*, 116−121.
(19) Zhang, W. W.; Huang, L. Q.; Zhu, J.; Liu, Y.; Wang, J. *Mater. Chem. Phys.* **2011**, *131*, 136−141.
(20) Fan, M. K.; Lai, F.-J.; Chou, H.-L.; Lu, W.-T.; Hwang, B.-J.; Brolo, A. G. *Chem. Sci.* **2013**, *4*, 509−515.
(21) Hao, E. C.; Schatza, G. C. *J. Chem. Phys.* **2004**, *120*, 357−366.
(22) Mallin, M. P.; Murphy, C. J. *Nano Lett.* **2002**, *2*, 1235−1237.
(23) Mulvaney, P. *Langmuir* **1996**, *12*, 788−800.
(24) Mallik, K.; Mandal, M.; Pradhan, N. *Nano Lett.* **2001**, *1*, 319−322.
(25) Fang, Y.; Li, Y.; Xu, H.; Sun, M. *Langmuir* **2010**, *26*, 7737−7746.
(26) Sun, M.; Xu, H. *Small* **2012**, *8*, 2777−2786.
(27) Ingram, D. B.; Christopher, P.; Bauer, J. L.; Linic, S. *ACS Catal.* **2011**, *1*, 1441−1447.
(28) Bzowski, A.; Kuhn, M.; Sham, T. K.; Rodriguez, J. A.; Hrbek, J. *Phys. Rev. B* **1999**, *59*, 13379−13393.
(29) Rycenga, M.; Hou, C. K. K.; Cobley, M.; Schwartz, A. G.; Camargo, P. H. C.; Xia, Y. *Phys. Chem. Chem. Phys.* **2009**, *11*, 5903−5908.